RESEARCH ARTICLE

WILEY

Functional connectivity gradients of the insula to different cerebral systems

Rui Wang[1,2,3] | **Fan Mo**[1,2,3] | **Yuhao Shen**[1,2,3] | **Yu Song**[1,2,3] |
Huanhuan Cai[1,2,3] | **Jiajia Zhu**[1,2,3] (ORCID)

[1]Department of Radiology, The First Affiliated Hospital of Anhui Medical University, Hefei, China

[2]Research Center of Clinical Medical Imaging, Anhui Province, Hefei, China

[3]Anhui Provincial Institute of Translational Medicine, Hefei, China

Correspondence
Jiajia Zhu, Department of Radiology, The First Affiliated Hospital of Anhui Medical University, No. 218, Jixi Road, Shushan District, Hefei 230022, China.
Email: zhujiajiagraduate@163.com

Abstract

The diverse functional roles of the insula may emerge from its heavy connectivity to an extensive network of cortical and subcortical areas. Despite several previous attempts to investigate the hierarchical organization of the insula by applying the recently developed gradient approach to insula-to-whole brain connectivity data, little is known about whether and how there is variability across connectivity gradients of the insula to different cerebral systems. Resting-state functional MRI data from 793 healthy subjects were used to discover and validate functional connectivity gradients of the insula, which were computed based on its voxel-wise functional connectivity profiles to distinct cerebral systems. We identified three primary patterns of functional connectivity gradients of the insula to distinct cerebral systems. The connectivity gradients to the higher-order transmodal associative systems, including the prefrontal, posterior parietal, temporal cortices, and limbic lobule, showed a ventroanterior-dorsal axis across the insula; those to the lower-order unimodal primary systems, including the motor, somatosensory, and occipital cortices, displayed radiating transitions from dorsoanterior toward both ventroanterior and dorsoposterior parts of the insula; the connectivity gradient to the subcortical nuclei exhibited an organization along the anterior–posterior axis of the insula. Apart from complementing and extending previous literature on the heterogeneous connectivity patterns of insula subregions, the presented framework may offer ample opportunities to refine our understanding of the role of the insula in many brain disorders.

KEYWORDS
resting-state functional MRI, insula, hierarchical organization, functional connectivity gradients

1 | INTRODUCTION

The insula lies folded deep within the lateral sulcus of each hemisphere, hidden below parts of the frontal, parietal, and temporal lobes (Gogolla, 2017; Uddin et al., 2017). It is a uniquely located, cytoarchitectonically complex, and richly connected brain structure that typically acts as an integration hub involved in a wide variety of functions ranging from lower-order sensorimotor processes to higher-order cognition and emotion (Benarroch, 2019; Centanni et al., 2021; Gasquoine, 2014; Gogolla, 2017; Menon & Uddin, 2010; Molnar-Szakacs & Uddin, 2022; Uddin et al., 2017). The diverse functional roles of the insula may emerge from its heavy connectivity to an

---

Rui Wang and Fan Mo contributed equally to this work.

extensive network of cortical and subcortical areas (Benarroch, 2019; Cauda et al., 2011; Cloutman et al., 2012; Gasquoine, 2014; Ghaziri et al., 2017; Gogolla, 2017; Taylor et al., 2009). Moreover, a large number of clinical neuroimaging studies have identified the insula as a core region affected across many psychiatric and neurological conditions including, but not limited to, autism (Lukito et al., 2020; Nomi et al., 2019; Uddin & Menon, 2009), schizophrenia (Qi et al., 2022; Sheffield et al., 2020; Xu et al., 2022; Zhu et al., 2015, 2017, 2018, 2020; Zhuo, Zhu, Qin, et al., 2017), depression (Kim & Han, 2021; Nord et al., 2021; Yu et al., 2020; Zhuo, Zhu, Wang, et al., 2017), addiction (Ghahremani et al., 2021; Perez Diaz et al., 2021; Qiu & Wang, 2021; Turel et al., 2021; Wei et al., 2017), anxiety disorders (Chavanne & Robinson, 2021; Cui et al., 2020; Feurer et al., 2021), Parkinson's disease (Carey et al., 2021; Pan et al., 2022; Tremblay et al., 2020), frontotemporal dementia (Gordon et al., 2016; Mandelli et al., 2016; Panman et al., 2019) and Alzheimer's disease (Jones et al., 2019; Liu et al., 2018; Nunez et al., 2020), highlighting its critical involvement in cross-disorder neuropathological mechanisms. Collectively, these empirical insights from brain structural and functional data have exposed the insula as an integral component of behavior in various non-disease and disease states, such that this brain structure has gained considerable attention in basic and clinical neuroscience.

On the basis of anatomy, connectivity, and functional contributions, the insula has been segmented into anywhere between 2 and 13 distinct subregions (Alcauter et al., 2015; Cauda et al., 2012; Centanni et al., 2021; Chang et al., 2013; Deen et al., 2011; Droutman et al., 2015; Faillenot et al., 2017; Ghaziri et al., 2018; Glasser et al., 2016; Kurth et al., 2010; Uddin et al., 2014; Uddin et al., 2017; Wysiadecki et al., 2018). At the simplest level, the insula is divided into anterior and posterior lobules by the central insular sulcus, with the anterior connected more to frontal and limbic areas and thus associated more with cognition and emotion, and the posterior connected more to motor and sensory areas and thus linked more with sensorimotor processes (Centanni et al., 2021; Faillenot et al., 2017; Uddin et al., 2017; Wysiadecki et al., 2018). Based on cytoarchitectonic analyses of the presence and density of cortical granular cell layer 4, the insula can be parsed into posterior granular, intermediate dysgranular, and anterior agranular subdivisions (Benarroch, 2019; Nieuwenhuys, 2012). Recently, more fine-grained segments of the insula have been obtained by using functional and structural connectivity-based parcellation techniques (Fan et al., 2016; Glasser et al., 2016; Nomi et al., 2016). It is noteworthy that most of these prior efforts have used data-driven segmentation and clustering algorithms to parcellate the insula into subregions, i.e., insula voxels that share similar features (e.g., cytoarchitecture or connectivity patterns) were clustered and each cluster is assumed to represent a putative insula subregion. Given the discordance in the number of insula subregions reported between earlier studies, no consensus has been reached yet on how many clusters comprise the insula (Cauda & Vercelli, 2013). Instead, one may argue that topographic heterogeneity in macroscale insula features may be parsimoniously characterized as a continuum of gradual change (Huntenburg et al., 2018), rather than with discrete and independent subregions.

Diverse and convergent evidence demonstrates the existence of hierarchical organization in multiscale brain structures, which is reflected in structure, function, connectivity, and gene expression (Bajada et al., 2017; Gomez et al., 2019; Guell et al., 2018; Huntenburg et al., 2017; Huntenburg et al., 2018; Kharabian Masouleh et al., 2020; Margulies et al., 2016; Marquand et al., 2017; Paquola et al., 2019; Shine et al., 2019; Vogel et al., 2020; Vos de Wael et al., 2018; Wagstyl et al., 2015; Yang et al., 2020). A recently proposed gradient approach has provided a critical framework for the characterization of brain hierarchical organization, i.e., applying dimensionality reduction techniques to high-dimensional brain features to obtain a parsimonious set of principal components that delineate continuous transitions of feature patterns across brain regions, referred to as gradients (Bajada et al., 2020; Hong et al., 2020; Vos de Wael et al., 2020). Several previous attempts, working within this framework, have been made to investigate the hierarchical principle of macroscale organization in the insula. For example, leveraging myelin-sensitive magnetic resonance imaging (MRI), Royer and colleagues found two myeloarchitecture gradients in the human insula, one running from ventral anterior to posterior banks and one radiating from dorsal anterior toward both ventral anterior and posterior subregions (Royer et al., 2020). Taking advantage of quantitative modeling of multi-shell diffusion MRI, Menon et al. identified insula microstructure gradients along its anterior–posterior and dorsal-ventral axes (Menon et al., 2020). Employing a combination of diffusion tensor imaging and probabilistic white matter tractography, Cerliani et al. revealed a rostrocaudal trajectory of anatomical connectivity variation in the human insula (Cerliani et al., 2012). A recent functional MRI (fMRI) study demonstrated that resting-state functional connectivity (rsFC) diversity of the insula could be most parsimoniously modeled as continuum of gradual change from dorsal-posterior to ventral-anterior, and interindividual variation in this continuum could explain significant variation in behavior (Tian & Zalesky, 2018). However, these studies constructed connectivity gradients of the insula based on its anatomical or functional connectivity to the whole brain, leaving open the question of whether and how there is variability across connectivity gradients of the insula to different cerebral systems.

To address this question, we used resting-state fMRI data from 793 healthy subjects to discover and validate functional connectivity gradients of the insula, which were computed based on its voxel-wise rsFC profiles to distinct cerebral systems. We hypothesized that functional connectivity gradients of the insula to cerebral systems with homogeneous features (e.g., lower-order unimodal systems) would show similar patterns, which would differ from those to systems with heterogeneous characteristics (e.g., higher-order transmodal systems).

2 | MATERIALS AND METHODS

2.1 | Participants

The study comprised a discovery dataset and two independent cross-scanner, cross-race validation datasets. The discovery participants
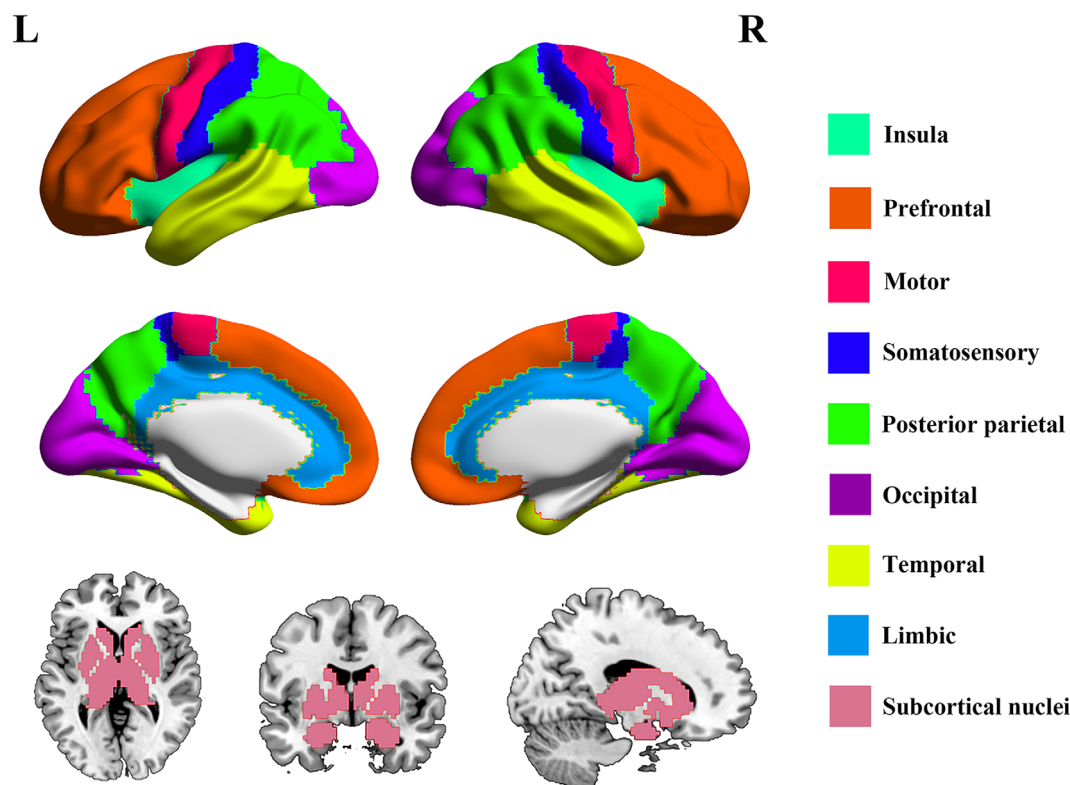
FIGURE 1 Illustration of the insula and other cerebral systems. Abbreviations: L, left; R, right

were a sample of healthy, right-handed Chinese Han adults, enrolled from the local universities and community via poster advertisements. Exclusion criteria included neuropsychiatric or severe somatic disorder, a history of head injury with consciousness loss, MRI contraindications, and a family history of psychiatric disease among first-degree relatives. This study was approved by the ethics committee of The First Affiliated Hospital of Anhui Medical University. Written informed consent was obtained from all participants after they had been given a complete description of the study. The validation samples were derived from two publicly available datasets: Consortium for Neuropsychiatric Phenomics (CNP, https://openneuro.org/datasets/ds000030/versions/1.0.0) (Poldrack et al., 2016) and Southwest University Adult Lifespan Dataset (SALD, https://doi.org/10.15387/fcp_indi.sald) (Wei et al., 2018). Notably, we solely selected the healthy adults from the cross-disorder CNP dataset. For the CNP dataset, healthy participants were excluded if they had lifetime diagnoses of psychiatric disorders, left handedness, pregnancy, or other contraindications to scanning; for the SALD dataset, the exclusion criteria included MRI contraindications, current psychiatric or neurological disorders, use of psychiatric drugs within 3 months, pregnancy, or a history of head trauma. Full details regarding the two validation samples (e.g., ethics, informed consent, inclusion, and exclusion criteria, among others) have been described in the previous studies (Poldrack et al., 2016; Wei et al., 2018). To exclude the potential influence of neurodevelopment and neurodegeneration, all the participants were restricted to an age range of 18–60 years. In addition, participants with poor image quality or excessive head motion during scanning

were excluded. This brought the final samples used in the current study to 361 (183 females) in the discovery dataset, 103 (47 females) in the CNP dataset, and 329 (207 females) in the SALD dataset. Demographic data of the three datasets are detailed in Table S1 in the Supplementary materials.

2.2 | MRI data acquisition

Resting-state functional MRI data of the discovery sample were acquired using the 3.0-Tesla General Electric Discovery MR750w scanner, and those of the validation samples were obtained using the 3.0-Tesla Siemens Trio scanners. Details of the acquisition parameters for the three datasets are shown in Table S2 in the Supplementary materials.

2.3 | Resting-state fMRI data preprocessing

Resting-state blood-oxygen-level-dependent (BOLD) data were preprocessed using Statistical Parametric Mapping (SPM12, http://www.fil.ion.ucl.ac.uk/spm) and Data Processing & Analysis for Brain Imaging (DPABI, http://rfmri.org/dpabi) (Yan et al., 2016). The first several brain volumes (discovery: 10, CNP: 5, SALD: 10) for each participant were discarded to allow the signal to reach equilibrium and the participants to adapt to scanning noise. The remaining volumes were corrected for the acquisition time delay between slices. Then,

realignment was performed to correct the motion between volumes. Head motion parameters were computed by estimating the translation in each direction and the angular rotation on each axis for each volume. All participants' BOLD data were within the defined motion thresholds (i.e., maximum translational or rotational motion parameters <2.0 mm or 2.0°). We also calculated frame-wise displacement (FD), which indexes the volume-to-volume changes in head position. Several nuisance covariates (the linear drift, the estimated motion parameters based on the Friston-24 model, the spike volumes with FD >0.5 mm, the white matter signal, and the cerebrospinal fluid signal) were regressed out from the data. Next, the datasets were band-pass filtered using a frequency range of 0.01 to 0.1 Hz. In the normalization step, individual high-resolution structural images were firstly co-registered with the mean functional images; then the transformed structural images were segmented and normalized to the Montreal Neurological Institute (MNI) space using the diffeomorphic anatomical registration through the exponentiated Lie algebra (DARTEL) technique (Ashburner, 2007). Finally, each filtered functional volume was spatially normalized to the MNI space using the deformation parameters estimated during the above step and resampled into a 3-mm cubic voxel.

2.4 | Definition of the insula and other cerebral systems

The Human Brainnetome Atlas (Fan et al., 2016) is a new brain atlas constructed using a connectivity-based parcellation framework, such that its brain regions are obtained based on their specific anatomical and functional connectivity patterns. We adopted this atlas to define the insula (965 voxels) and other eight cerebral systems. Specifically, the prefrontal cortex (10,667 voxels) comprises the superior frontal, middle frontal, inferior frontal, and orbitofrontal gyri; the motor cortex (2492 voxels) consists of the precentral gyrus and anterior portion of the paracentral lobule; the somatosensory cortex (1962 voxels) includes the postcentral gyrus and posterior portion of the paracentral lobule; the posterior parietal cortex (7076 voxels) comprises the superior parietal lobule, inferior parietal lobule, and precuneus; the occipital cortex (5157 voxels) consists of the medioventral occipital and lateral occipital cortices; the temporal cortex (8209 voxels) includes the superior temporal, middle temporal, inferior temporal, fusiform, and parahippocampal gyri as well as posterior superior temporal sulcus; the limbic lobule (1661 voxels) refers to the cingulate gyrus; the subcortical nuclei (3234 voxels) comprises the amygdala, hippocampus, basal ganglia, and thalamus (Figure 1 and Table S3 in the Supplementary materials).

2.5 | Calculation of functional connectivity gradients

A schematic overview of the calculating procedure of functional connectivity gradients of the insula is presented in Figure 2. Functional connectivity gradients were calculated based on rsFC of the insula to the other eight cerebral systems. First, the preprocessed BOLD images were concatenated across all subjects after standardization using z-scores, yielding group-level BOLD time courses. Second, for each cerebral system, a voxel-wise insula-to-cerebral system rsFC matrix was generated by calculating Pearson's correlation coefficients between group-level BOLD time courses of each voxel within the insula and each voxel within that cerebral system. The resultant eight rsFC matrices (insula-to-prefrontal cortex: $965 \times 10,667$; insula-to-motor cortex: 965×2492; insula-to-somatosensory cortex: 965×1962; insula-to-posterior parietal cortex: 965×7076; insula-to-occipital cortex: 965×5157; insula-to-temporal cortex: 965×8209; insula-to-limbic lobule: 965×1661; insula-to-subcortical nuclei: 965×3234) were Fisher's Z-transformed to improve normality. Then, for each row in the rsFC matrix, the top 10% rsFC values were retained, whereas all others were set to zeros (Margulies et al., 2016; Yang et al., 2020). Third, similarity between all pairs of rows was calculated using cosine distance, yielding a positive symmetric affinity matrix (965×965) reflecting similarity of rsFC profiles between each pair of voxels within the insula.

We calculated functional connectivity gradients using diffusion map embedding (Coifman et al., 2005; Guell et al., 2018; Margulies et al., 2016), a nonlinear dimensionality reduction technique that can recover a low-dimensional embedding from high-dimensional connectivity data. In the embedding space, voxels that are strongly connected by either many connections or few very strong connections are close, whereas voxels with little or no connections are far apart. Compared with other non-linear dimensionality reduction algorithms, diffusion map embedding is relatively robust to noise, computationally inexpensive, and provides a stable representation of connections (Lafon & Lee, 2016). By applying this algorithm to each affinity matrix, we identified multiple low-dimensional gradients accounting for connectivity variance in descending order. For each gradient, a gradient value (normalized using z-scores) was assigned to each voxel within the insula, resulting in an insula gradient map to visualize macroscale continuous transitions in overall connectivity patterns, i.e., the gradient topography. We focused on the first gradient (i.e., the principal gradient) that explained the greatest variance in connectivity. Notably, the diffusion map embedding is controlled by a single parameter α, which controls the influence of the density of sampling points on the underlying manifold ($\alpha = 0$, maximal influence; $\alpha = 1$, no influence). Following previous studies (Dong et al., 2020; Guell et al., 2018; Hong et al., 2019; Margulies et al., 2016; Yang et al., 2020), we set $\alpha = 0.5$ that is considered well-suited for the analysis of brain connectivity data.

2.6 | Validation analyses

Several validation analyses were conducted to verify the robustness of our results. First, our main analyses were performed in the discovery dataset. To exclude the influence of samples, we repeated the above-described analyses in two independent cross-race, cross-
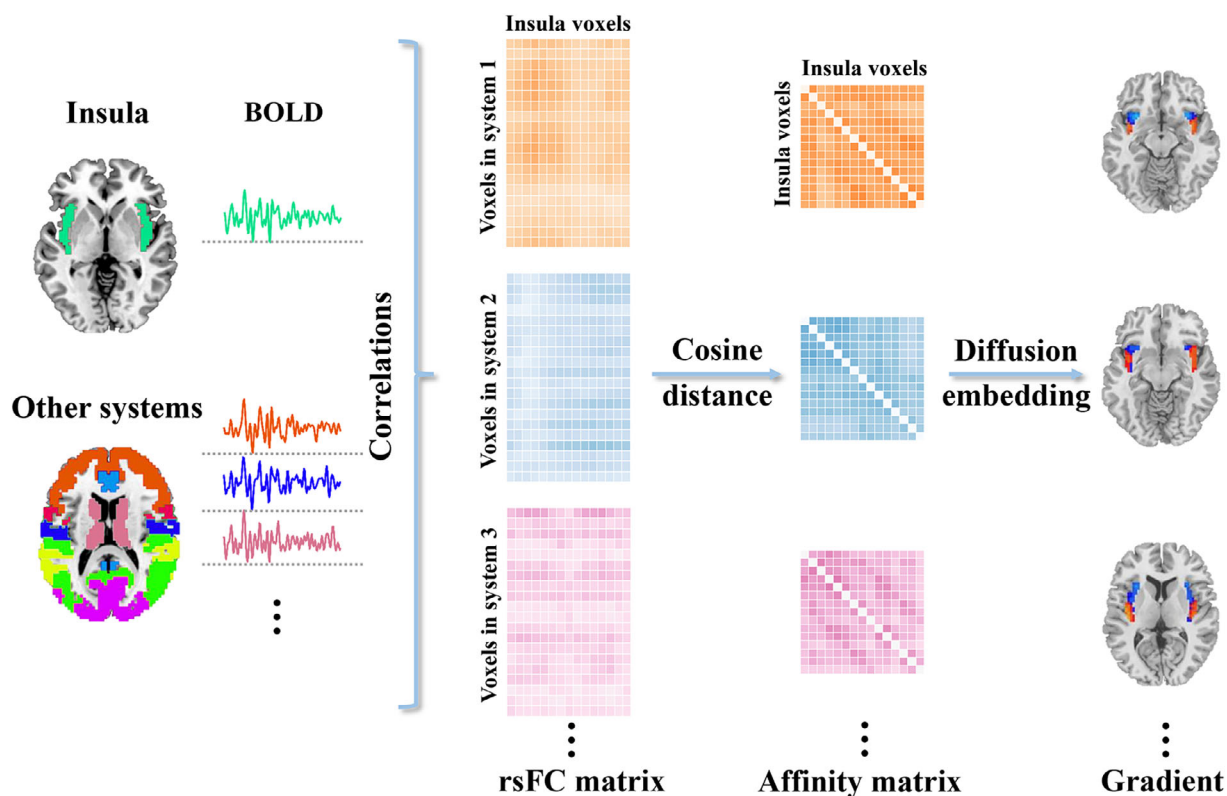
FIGURE 2 Calculating procedure of functional connectivity gradients of the insula. For each cerebral system, a voxel-wise insula-to-cerebral system rsFC matrix was generated by calculating Pearson's correlation coefficients between BOLD time courses of each voxel within the insula and each voxel within that cerebral system. For each resultant rsFC matrix, similarity between all pairs of rows was calculated using cosine distance, yielding a positive symmetric affinity matrix reflecting similarity of rsFC profiles between each pair of voxels within the insula. Functional connectivity gradients were then calculated using diffusion map embedding. For each cerebral system, we focused on the first gradient that explained the greatest connectivity variance and a gradient value was assigned to each voxel within the insula, generating an insula gradient map to visualize the gradient topography. Abbreviations: BOLD, blood-oxygen-level-dependent; rsFC, resting-state functional connectivity

scanner validation datasets (CNP and SALD). Second, before calculating the affinity matrix, we retained the top 10% rsFC values per row in the rsFC matrix. To examine the effect of threshold selections, we re-ran our analysis with use of two other thresholds (top 20% and 30%). Finally, global signal regression (GSR) has been a controversial step in the preprocessing of resting-state fMRI data (Murphy & Fox, 2017). To assess its potential impact, we re-computed the rsFC matrix based on BOLD data with GSR and then repeated the functional connectivity gradient analyses.

3 | RESULTS

3.1 | Functional connectivity gradients of the insula

Functional connectivity gradients of the insula presented distinct topographies along with different degrees of explained connectivity variance across cerebral systems, which could be summarized as three primary patterns. The first pattern was observed for the functional connectivity gradients of the insula to the higher-order transmodal associative systems including the prefrontal, posterior parietal, temporal cortices, and limbic lobule, which accounted for a high degree of connectivity variance (53%–60%). This pattern showed a ventroanterior-dorsal axis across the insula, characterized by a gradual change from ventroanterior to dorsal portion (Figure 3). The second pattern was found for the functional connectivity gradients of the insula to the lower-order unimodal primary systems including the motor, somatosensory, and occipital cortices, which explained a moderate degree of connectivity variance (23%–31%). This pattern displayed radiating transitions from dorsoanterior toward both ventroanterior and dorsoposterior parts of the insula (Figure 4). The third pattern was seen for the functional connectivity gradient of the insula to the subcortical nuclei, which accounted for a relatively low degree of connectivity variance (20%). This pattern exhibited an organization along the anterior–posterior axis, characterized by a gradual change from anterior to posterior portion of the insula (Figure 5). Scree plots showing the connectivity variance explained by the gradients of the insula to the eight cerebral systems are provided in Figure S1 in the Supplementary materials.
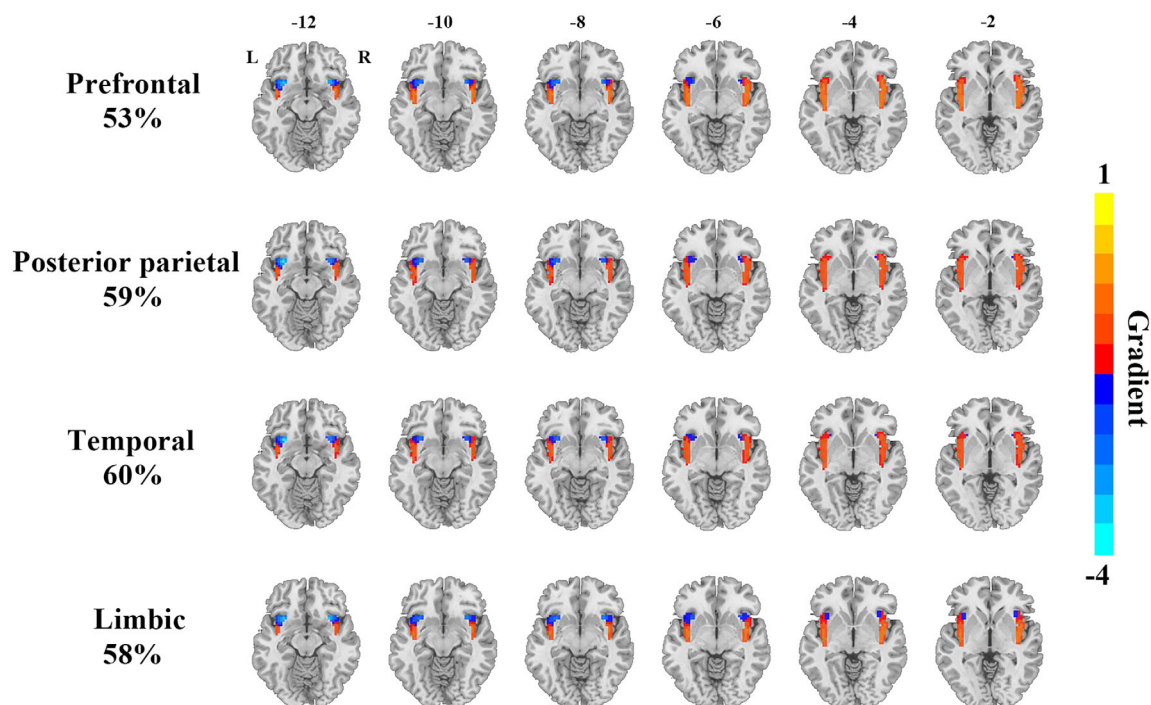
FIGURE 3 Functional connectivity gradients of the insula to the higher-order transmodal associative systems including the prefrontal, posterior parietal, temporal cortices and limbic lobule. The percentages represent connectivity variance explained by the corresponding gradients. Abbreviations: L, left; R, right
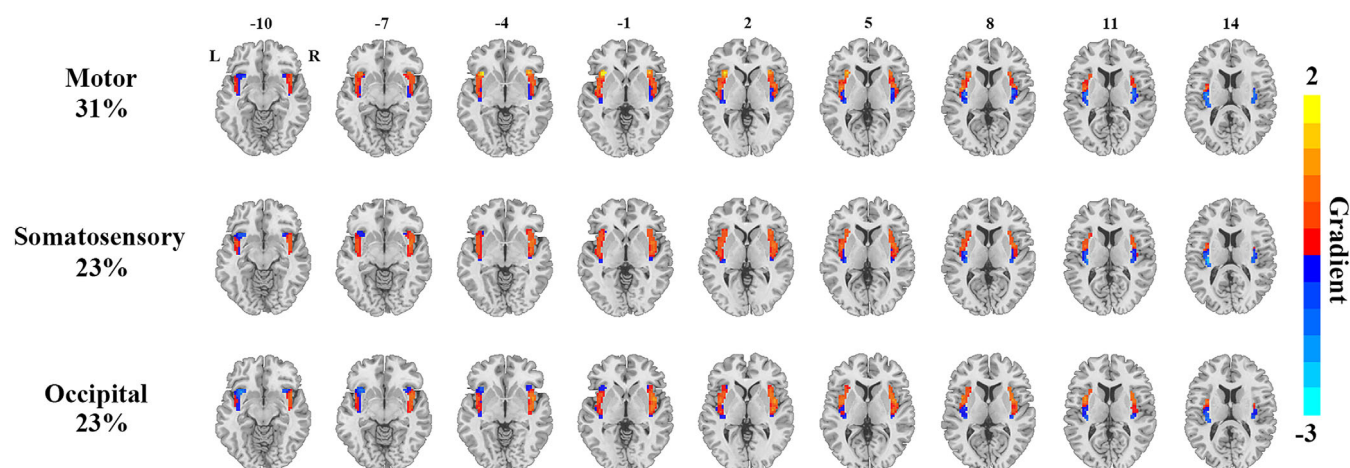

FIGURE 4 Functional connectivity gradients of the insula to the lower-order unimodal primary systems including the motor, somatosensory, and occipital cortices. The percentages represent connectivity variance explained by the corresponding gradients. Abbreviations: L, left; R, right

3.2 | Validation analyses

The results of validation analyses supported the robustness of our findings. First, the insula functional connectivity gradients derived from two independent cross-race, cross-scanner validation datasets (CNP and SALD) were largely consistent with those from the discovery dataset (Figures S2–S4 in the Supplementary materials), indicating no influence of samples. Second, when applying two other thresholds (top 20% and 30%) to the rsFC matrix, we found

that explained connectivity variance and topographies of the insula functional connectivity gradients were nearly identical to those using the threshold of top 10% (Figures S5–S7 in the Supplementary materials), suggesting no effect of threshold selections. Finally, analyzing BOLD data with GSR yielded insula functional connectivity gradients similar to those in our main analysis of BOLD data without GSR, with exception of the insula-to-motor cortex and insula-to-subcortical nuclei gradients (Figures S8–S10 in the Supplementary materials).
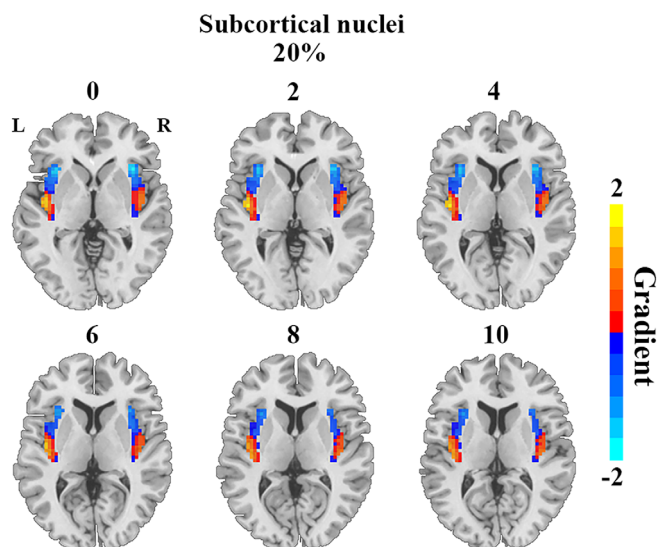
Subcortical nuclei
20%

FIGURE 5 Functional connectivity gradient of the insula to the subcortical nuclei. The percentage represents connectivity variance explained by the gradient. Abbreviations: L, left; R, right

4 | DISCUSSION

The insula has long been considered a key cortical hub with widespread connectivity to a rich range of cortical and subcortical regions serving sensorimotor, emotional, and cognitive processes, which gives rise to its diverse functional roles (Benarroch, 2019; Centanni et al., 2021; Chen et al., 2018; Gasquoine, 2014; Gogolla, 2017; He et al., 2019; Menon & Uddin, 2010; Molnar-Szakacs & Uddin, 2022; Uddin et al., 2017). For instance, it is well established that the insula has a wide array of connections with the prefrontal, motor, somatosensory, posterior parietal, occipital, and temporal cortices as well as limbic lobule and subcortical nuclei (Benarroch, 2019; Cauda et al., 2011; Cloutman et al., 2012; Gasquoine, 2014; Ghaziri et al., 2017; Gogolla, 2017; Taylor et al., 2009). From a network perspective, the insula functions as a causal outflow hub within the salience network that permits controls of network dynamics through direct and indirect links to important nodes within major networks including the central executive, default mode, dorsal attention, ventral attention, sensorimotor, visual, and auditory networks (Cauda et al., 2011; Centanni et al., 2021; Menon & Uddin, 2010; Molnar-Szakacs & Uddin, 2022). Crucially, there is solid evidence that different insula subregions show distinct structural and functional connectivity patterns (Alcauter et al., 2015; Cauda et al., 2012; Centanni et al., 2021; Chang et al., 2013; Deen et al., 2011; Fan et al., 2016; Ghaziri et al., 2017; Ghaziri et al., 2018; Glasser et al., 2016; Nomi et al., 2016). Altogether, this previous literature has led to some speculation that there may be heterogeneous hierarchical organizations within the insula reflecting its connectivity profiles to different cerebral systems.

The high-dimensionality of brain connectivity data lies in the fact that each brain location has more than one connection. In this context, dimensionality reduction techniques are required to extract intelligible information from such high-dimensional connectivity data. One commonly used method is to group brain locations into larger parcels based on connectivity similarity, i.e., clustering-based parcellation of insula subregions. Nevertheless, treating subregions as discrete and independent entities cannot characterize more gradual changes and overarching spatial relationships (Jbabdi et al., 2013). Instead, the recently developed gradient approach finds the main axes of variance in the data through decomposition or embedding algorithms, and replaces the original high dimensions of connectivity data with a more parsimonious set of new dimensions (i.e., connectivity gradients) that account for most of the connectivity variance. Each gradient is a continuous representation of one aspect of insula connectivity hierarchy, and each brain location can be quantified by a value reflective of where it falls along this gradient. Extensive research has established that the spatial arrangement of brain locations along these connectivity gradients is not arbitrary, but rather a consequence of developmental mechanisms shaped through evolutionary selection (Huntenburg et al., 2018). Combined, a gradient-based rather than cluster-based conceptualization may facilitate a more thorough characterization of the hierarchical organization of insula connectivity.

By applying Laplacian eigenmaps to anatomical connectivity data derived from diffusion tensor imaging and probabilistic white matter tractography, Cerliani et al. revealed a rostrocaudal trajectory of anatomical connectivity variability ranging from anterior dorsal and ventral to dorsal caudal part of the insula (Cerliani et al., 2012). Likewise, application of Laplacian eigenmaps to functional connectivity data from resting-state fMRI revealed that rsFC diversity across the insula's topography could be parsimoniously modeled as continuum of gradual change from dorsal-posterior to ventral-anterior; moreover, interindividual variation in insula functional connectivity gradients could account for inter-individual difference in behavior (Tian & Zalesky, 2018), and insula functional connectivity gradients were altered in individuals with schizophrenia and related to clinical symptoms of this disorder (Tian et al., 2019). Despite these prior investigations demonstrating the potential usefulness of the gradient approach in delineating the hierarchical organization of insula connectivity in health and disease, their gradients were constructed based on insula-to-whole brain connectivity data, which may overlook the heterogeneity in connectivity profiles of the insula to different cerebral systems.

The current study opens new perspectives by being the first to examine functional connectivity gradients of the insula to distinct cerebral systems, and identified three primary patterns of connectivity gradients. In agreement with our expectations, the functional connectivity gradients to the higher-order transmodal associative systems, including the prefrontal, posterior parietal, temporal cortices and limbic lobule, showed a ventroanterior-dorsal axis across the insula; those to the lower-order unimodal primary systems, including the motor, somatosensory, and occipital cortices, displayed radiating transitions from dorsoanterior toward both ventroanterior and dorsoposterior parts of the insula; the functional connectivity gradient to the

subcortical nuclei exhibited an organization along the anterior–posterior axis of the insula. The observed topographies of insula connectivity gradients at the system level are partially consistent with those based on insula-to-whole brain connectivity reported in prior studies (Cerliani et al., 2012; Tian et al., 2019; Tian & Zalesky, 2018), suggesting that the latter likely involve some mixture of the former and thus may obscure specificity. More importantly, our data complement and extend previous literature on the heterogeneous connectivity patterns of insula subregions (Alcauter et al., 2015; Cauda et al., 2012; Centanni et al., 2021; Chang et al., 2013; Deen et al., 2011; Fan et al., 2016; Ghaziri et al., 2017, 2018; Glasser et al., 2016; Nomi et al., 2016; Zhao et al., 2022), by demonstrating that the connectivity heterogeneity of the insula can also be captured by its topographic organizations.

This study has several limitations that should be addressed in future work. First, to obtain more stable and reliable results, functional connectivity gradients of the insula were calculated at the group level rather than at the individual level, which may obscure meaningful inter-individual differences. Second, we focused our analyses on the first gradient that accounted for the greatest variance in connectivity. Nevertheless, some physiologically significant gradients with smaller explained variance may be overlooked, hampering the possibility to achieve a more fruitful characterization of the insula functional connectivity hierarchy. Third, the cerebral systems were defined using the Human Brainnetome Atlas. Some data-driven approaches, e.g., independent component analysis, have been adopted to define functional networks, which are considered more functionally homogeneous and may be better at capturing individual differences of real functional boundaries than those defined by existing atlases (Calhoun et al., 2001). Therefore, our results should be validated in further studies utilizing data-driven parcellation approaches. Finally, since the resting-state fMRI field-of-view did not include the entire cerebellum in all subjects, we only calculated functional connectivity gradients of the insula to the cerebral systems, leaving the insula-to-cerebellum functional connectivity gradients elusive.

In conclusion, using a combination of resting-state fMRI and functional connectivity gradients, we established three different topographic patterns of the insula reflecting its rsFC profiles to the higher-order transmodal associative, lower-order unimodal primary, and subcortical systems. Apart from complementing and extending previous literature on the heterogeneous connectivity patterns of insula subregions, the presented framework may offer ample opportunities to refine our understanding of the role of the insula in many brain disorders, e.g., quantifying patient-specific deviations from normative gradients and relating these gradients to diagnostic labels, clinical symptoms, and cognitive impairments.

DATA AVAILABILITY STATEMENT

The data that support the findings of this study are available on request from the corresponding author. The data are not publicly available due to privacy or ethical restrictions.

ORCID

Jiajia Zhu https://orcid.org/0000-0001-7343-6241

REFERENCES

Alcauter, S., Lin, W., Keith Smith, J., Gilmore, J. H., & Gao, W. (2015). Consistent anterior-posterior segregation of the insula during the first 2 years of life. *Cerebral Cortex*, *25*(5), 1176–1187. https://doi.org/10.1093/cercor/bht312

Ashburner, J. (2007). A fast diffeomorphic image registration algorithm. *NeuroImage*, *38*(1), 95–113. https://doi.org/10.1016/j.neuroimage.2007.07.007

Bajada, C. J., Costa Campos, L. Q., Caspers, S., Muscat, R., Parker, G. J. M., Lambon Ralph, M. A., Cloutman, L. L., & Trujillo-Barreto, N. J. (2020). A tutorial and tool for exploring feature similarity gradients with MRI data. *NeuroImage*, *221*, 117140. https://doi.org/10.1016/j.neuroimage.2020.117140

Bajada, C. J., Jackson, R. L., Haroon, H. A., Azadbakht, H., Parker, G. J. M., Lambon Ralph, M. A., & Cloutman, L. L. (2017). A graded tractographic parcellation of the temporal lobe. *NeuroImage*, *155*, 503–512. https://doi.org/10.1016/j.neuroimage.2017.04.016

Benarroch, E. E. (2019). Insular cortex: Functional complexity and clinical correlations. *Neurology*, *93*(21), 932–938. https://doi.org/10.1212/WNL.0000000000008525

Carey, G., Gormezoglu, M., de Jong, J. J. A., Hofman, P. A. M., Backes, W. H., Dujardin, K., & Leentjens, A. F. G. (2021). Neuroimaging of anxiety in Parkinson's Disease: A systematic review. *Movement Disorders*, *36*(2), 327–339. https://doi.org/10.1002/mds.28404

Cauda, F., Costa, T., Torta, D. M., Sacco, K., D'Agata, F., Duca, S., Geminiani, G., Fox, P. T., & Vercelli, A. (2012). Meta-analytic clustering of the insular cortex: Characterizing the meta-analytic connectivity of the insula when involved in active tasks. *NeuroImage*, *62*(1), 343–355. https://doi.org/10.1016/j.neuroimage.2012.04.012

Cauda, F., D'Agata, F., Sacco, K., Duca, S., Geminiani, G., & Vercelli, A. (2011). Functional connectivity of the insula in the resting brain. *NeuroImage*, *55*(1), 8–23. https://doi.org/10.1016/j.neuroimage.2010.11.049

Cauda, F., & Vercelli, A. (2013). How many clusters in the insular cortex? *Cerebral Cortex*, *23*(11), 2779–2780. https://doi.org/10.1093/cercor/bhs249

Centanni, S. W., Janes, A. C., Haggerty, D. L., Atwood, B., & Hopf, F. W. (2021). Better living through understanding the insula: Why subregions can make all the difference. *Neuropharmacology*, *198*, 108765. https://doi.org/10.1016/j.neuropharm.2021.108765

Cerliani, L., Thomas, R. M., Jbabdi, S., Siero, J. C., Nanetti, L., Crippa, A., Gazzola, V., D'Arceuil, H., & Keysers, C. (2012). Probabilistic tractography recovers a rostrocaudal trajectory of connectivity variability in the human insular cortex. *Human Brain Mapping*, *33*(9), 2005–2034. https://doi.org/10.1002/hbm.21338

Chang, L. J., Yarkoni, T., Khaw, M. W., & Sanfey, A. G. (2013). Decoding the role of the insula in human cognition: Functional parcellation and large-scale reverse inference. *Cerebral Cortex*, *23*(3), 739–749. https://doi.org/10.1093/cercor/bhs065

Chavanne, A. V., & Robinson, O. J. (2021). The overlapping neurobiology of induced and pathological anxiety: A meta-analysis of functional

neural activation. *The American Journal of Psychiatry*, *178*(2), 156–164. https://doi.org/10.1176/appi.ajp.2020.19111153

Chen, R., Li, D. P., Turel, O., Sorensen, T. A., Bechara, A., Li, Y., & He, Q. (2018). Decision making deficits in relation to food cues influence obesity: A triadic neural model of problematic eating. *Frontiers in Psychiatry*, *9*, 264. https://doi.org/10.3389/fpsyt.2018.00264

Cloutman, L. L., Binney, R. J., Drakesmith, M., Parker, G. J., & Lambon Ralph, M. A. (2012). The variation of function across the human insula mirrors its patterns of structural connectivity: Evidence from in vivo probabilistic tractography. *NeuroImage*, *59*(4), 3514–3521. https://doi.org/10.1016/j.neuroimage.2011.11.016

Coifman, R. R., Lafon, S., Lee, A. B., Maggioni, M., Nadler, B., Warner, F., & Zucker, S. W. (2005). Geometric diffusions as a tool for harmonic analysis and structure definition of data: Multiscale methods. *PNAS*, *102*(21), 7432–7437.

Cui, H., Zhang, B., Li, W., Li, H., Pang, J., Hu, Q., Zhang, L., Tang, Y., Yang, Z., Wang, J., Li, C., & Northoff, G. (2020). Insula shows abnormal task-evoked and resting-state activity in first-episode drug-naive generalized anxiety disorder. *Depression and Anxiety*, *37*(7), 632–644. https://doi.org/10.1002/da.23009

Deen, B., Pitskel, N. B., & Pelphrey, K. A. (2011). Three systems of insular functional connectivity identified with cluster analysis. *Cerebral Cortex*, *21*(7), 1498–1506. https://doi.org/10.1093/cercor/bhq186

Dong, D., Luo, C., Guell, X., Wang, Y., He, H., Duan, M., Eickhoff, S. B., & Yao, D. (2020). Compression of cerebellar functional gradients in schizophrenia. *Schizophrenia Bulletin*, *46*, 1282–1295. https://doi.org/10.1093/schbul/sbaa016

Droutman, V., Bechara, A., & Read, S. J. (2015). Roles of the different subregions of the insular cortex in various phases of the decision-making process. *Frontiers in Behavioral Neuroscience*, *9*, 309. https://doi.org/10.3389/fnbeh.2015.00309

Faillenot, I., Heckemann, R. A., Frot, M., & Hammers, A. (2017). Macroanatomy and 3D probabilistic atlas of the human insula. *NeuroImage*, *150*, 88–98. https://doi.org/10.1016/j.neuroimage.2017.01.073

Fan, L., Li, H., Zhuo, J., Zhang, Y., Wang, J., Chen, L., Yang, Z., Chu, C., Xie, S., Laird, A. R., Fox, P. T., Eickhoff, S. B., Yu, C., & Jiang, T. (2016). The human Brainnetome atlas: A new brain atlas based on connectional architecture. *Cerebral Cortex*, *26*(8), 3508–3526. https://doi.org/10.1093/cercor/bhw157

Feurer, C., Suor, J. H., Jimmy, J., Klumpp, H., Monk, C. S., Phan, K. L., & Burkhouse, K. L. (2021). Differences in cortical thinning across development among individuals with and without anxiety disorders. *Depression and Anxiety*, *38*(3), 372–381. https://doi.org/10.1002/da.23096

Gasquoine, P. G. (2014). Contributions of the insula to cognition and emotion. *Neuropsychology Review*, *24*(2), 77–87. https://doi.org/10.1007/s11065-014-9246-9

Ghahremani, D. G., Pochon, J. B., Perez Diaz, M., Tyndale, R. F., Dean, A. C., & London, E. D. (2021). Functional connectivity of the anterior insula during withdrawal from cigarette smoking. *Neuropsychopharmacology*, *46*(12), 2083–2089. https://doi.org/10.1038/s41386-021-01036-z

Ghaziri, J., Tucholka, A., Girard, G., Boucher, O., Houde, J. C., Descoteaux, M., Obaid, S., Gilbert, G., Rouleau, I., & Nguyen, D. K. (2018). Subcortical structural connectivity of insular subregions. *Scientific Reports*, *8*(1), 8596. https://doi.org/10.1038/s41598-018-26995-0

Ghaziri, J., Tucholka, A., Girard, G., Houde, J. C., Boucher, O., Gilbert, G., Descoteaux, M., Lippe, S., Rainville, P., & Nguyen, D. K. (2017). The Corticocortical structural connectivity of the human insula. *Cerebral Cortex*, *27*(2), 1216–1228. https://doi.org/10.1093/cercor/bhv308

Glasser, M. F., Coalson, T. S., Robinson, E. C., Hacker, C. D., Harwell, J., Yacoub, E., Ugurbil, K., Andersson, J., Beckmann, C. F., Jenkinson, M., Smith, S. M., & Van Essen, D. C. (2016). A multi-modal parcellation of human cerebral cortex. *Nature*, *536*(7615), 171–178. https://doi.org/10.1038/nature18933

Gogolla, N. (2017). The insular cortex. *Current Biology*, *27*(12), R580–R586. https://doi.org/10.1016/j.cub.2017.05.010

Gomez, J., Zhen, Z., & Weiner, K. S. (2019). Human visual cortex is organized along two genetically opposed hierarchical gradients with unique developmental and evolutionary origins. *PLoS Biology*, *17*(7), e3000362. https://doi.org/10.1371/journal.pbio.3000362

Gordon, E., Rohrer, J. D., & Fox, N. C. (2016). Advances in neuroimaging in frontotemporal dementia. *Journal of Neurochemistry*, *138*(Suppl 1), 193–210. https://doi.org/10.1111/jnc.13656

Guell, X., Schmahmann, J. D., Gabrieli, J., & Ghosh, S. S. (2018). Functional gradients of the cerebellum. *eLife*, *7*, e36652. https://doi.org/10.7554/eLife.36652

He, Q., Huang, X., Zhang, S., Turel, O., Ma, L., & Bechara, A. (2019). Dynamic causal modeling of insular, striatal, and prefrontal cortex activities during a food-specific go/NoGo task. *Biological Psychiatry: Cognitive Neuroscience and Neuroimaging*, *4*(12), 1080–1089. https://doi.org/10.1016/j.bpsc.2018.12.005

Hong, S. J., Vos de Wael, R., Bethlehem, R. A. I., Lariviere, S., Paquola, C., Valk, S. L., Milham, M. P., Di Martino, A., Margulies, D. S., Smallwood, J., & Bernhardt, B. C. (2019). Atypical functional connectome hierarchy in autism. *Nature Communications*, *10*(1), 1022. https://doi.org/10.1038/s41467-019-08944-1

Hong, S. J., Xu, T., Nikolaidis, A., Smallwood, J., Margulies, D. S., Bernhardt, B., Vogelstein, J., & Milham, M. P. (2020). Toward a connectivity gradient-based framework for reproducible biomarker discovery. *NeuroImage*, *223*, 117322. https://doi.org/10.1016/j.neuroimage.2020.117322

Huntenburg, J. M., Bazin, P. L., Goulas, A., Tardif, C. L., Villringer, A., & Margulies, D. S. (2017). A systematic relationship between functional connectivity and Intracortical myelin in the human cerebral cortex. *Cerebral Cortex*, *27*(2), 981–997. https://doi.org/10.1093/cercor/bhx030

Huntenburg, J. M., Bazin, P. L., & Margulies, D. S. (2018). Large-scale gradients in human cortical organization. *Trends in Cognitive Sciences*, *22*(1), 21–31. https://doi.org/10.1016/j.tics.2017.11.002

Jbabdi, S., Sotiropoulos, S. N., & Behrens, T. E. (2013). The topographic connectome. *Current Opinion in Neurobiology*, *23*(2), 207–215. https://doi.org/10.1016/j.conb.2012.12.004

Jones, S. A., De Marco, M., Manca, R., Bell, S. M., Blackburn, D. J., Wilkinson, I. D., Soininen, H., & Venneri, A. (2019). Altered frontal and insular functional connectivity as pivotal mechanisms for apathy in Alzheimer's disease. *Cortex*, *119*, 100–110. https://doi.org/10.1016/j.cortex.2019.04.008

Kharabian Masouleh, S., Plachti, A., Hoffstaedter, F., Eickhoff, S., & Genon, S. (2020). Characterizing the gradients of structural covariance in the human hippocampus. *NeuroImage*, *218*, 116972. https://doi.org/10.1016/j.neuroimage.2020.116972

Kim, Y. K., & Han, K. M. (2021). Neural substrates for late-life depression: A selective review of structural neuroimaging studies. *Progress in Neuro-Psychopharmacology & Biological Psychiatry*, *104*, 110010. https://doi.org/10.1016/j.pnpbp.2020.110010

Kurth, F., Zilles, K., Fox, P. T., Laird, A. R., & Eickhoff, S. B. (2010). A link between the systems: Functional differentiation and integration within the human insula revealed by meta-analysis. *Brain Structure & Function*, *214*(5–6), 519–534. https://doi.org/10.1007/s00429-010-0255-z

Lafon, S., & Lee, A. B. (2016). Diffusion maps and coarse-graining a unified framework for dimensionality reduction, graph partitioning, and data set parameterization. *IEEE Transactions on Pattern Analysis and Machine Intelligence*, *28*, 1393–1403. https://doi.org/10.1109/TPAMI.2006.184

Liu, X., Chen, X., Zheng, W., Xia, M., Han, Y., Song, H., Li, K., He, Y., & Wang, Z. (2018). Altered functional connectivity of insular subregions in Alzheimer's Disease. *Frontiers in Aging Neuroscience*, *10*, 107. https://doi.org/10.3389/fnagi.2018.00107

Lukito, S., Norman, L., Carlisi, C., Radua, J., Hart, H., Simonoff, E., & Rubia, K. (2020). Comparative meta-analyses of brain structural and

functional abnormalities during cognitive control in attention-deficit/hyperactivity disorder and autism spectrum disorder. *Psychological Medicine*, *50*(6), 894–919. https://doi.org/10.1017/S0033291720000574

Mandelli, M. L., Vitali, P., Santos, M., Henry, M., Gola, K., Rosenberg, L., Dronkers, N., Miller, B., Seeley, W. W., & Gorno-Tempini, M. L. (2016). Two insular regions are differentially involved in behavioral variant FTD and nonfluent/agrammatic variant PPA. *Cortex*, *74*, 149–157. https://doi.org/10.1016/j.cortex.2015.10.012

Margulies, D. S., Ghosh, S. S., Goulas, A., Falkiewicz, M., Huntenburg, J. M., Langs, G., Bezgin, G., Eickhoff, S. B., Castellanos, F. X., Petrides, M., Jefferies, E., & Smallwood, J. (2016). Situating the default-mode network along a principal gradient of macroscale cortical organization. *Proceedings of the National Academy of Sciences of the United States of America*, *113*(44), 12574–12579. https://doi.org/10.1073/pnas.1608282113

Marquand, A. F., Haak, K. V., & Beckmann, C. F. (2017). Functional corti-costriatal connection topographies predict goal directed behaviour in humans. *Nature Human Behaviour*, *1*(8), 146. https://doi.org/10.1038/s41562-017-0146

Menon, V., Gallardo, G., Pinsk, M. A., Nguyen, V. D., Li, J. R., Cai, W., & Wassermann, D. (2020). Microstructural organization of human insula is linked to its macrofunctional circuitry and predicts cognitive control. *eLife*, *9*, 9. https://doi.org/10.7554/eLife.53470

Menon, V., & Uddin, L. Q. (2010). Saliency, switching, attention and control: A network model of insula function. *Brain Structure & Function*, *214*(5–6), 655–667. https://doi.org/10.1007/s00429-010-0262-0

Molnar-Szakacs, I., & Uddin, L. Q. (2022). Anterior insula as a gatekeeper of executive control. *Neuroscience and Biobehavioral Reviews*, *139*, 104736. https://doi.org/10.1016/j.neubiorev.2022.104736

Murphy, K., & Fox, M. D. (2017). Towards a consensus regarding global signal regression for resting state functional connectivity MRI. *NeuroImage*, *154*, 169–173. https://doi.org/10.1016/j.neuroimage.2016.11.052

Nieuwenhuys, R. (2012). The insular cortex: A review. *Progress in Brain Research*, *195*, 123–163. https://doi.org/10.1016/B978-0-444-53860-4.00007-6

Nomi, J. S., Farrant, K., Damaraju, E., Rachakonda, S., Calhoun, V. D., & Uddin, L. Q. (2016). Dynamic functional network connectivity reveals unique and overlapping profiles of insula subdivisions. *Human Brain Mapping*, *37*(5), 1770–1787. https://doi.org/10.1002/hbm.23135

Nomi, J. S., Molnar-Szakacs, I., & Uddin, L. Q. (2019). Insular function in autism: Update and future directions in neuroimaging and interventions. *Progress in Neuro-Psychopharmacology & Biological Psychiatry*, *89*, 412–426. https://doi.org/10.1016/j.pnpbp.2018.10.015

Nord, C. L., Lawson, R. P., & Dalgleish, T. (2021). Disrupted dorsal mid-insula activation during Interoception across psychiatric disorders. *The American Journal of Psychiatry*, *178*(8), 761–770. https://doi.org/10.1176/appi.ajp.2020.20091340

Nunez, C., Callen, A., Lombardini, F., Compta, Y., Stephan-Otto, C., & Alzheimer's Disease Neuroimaging, I. (2020). Different cortical Gyrification patterns in Alzheimer's Disease and impact on memory performance. *Annals of Neurology*, *88*(1), 67–80. https://doi.org/10.1002/ana.25741

Pan, C., Ren, J., Li, L., Li, Y., Xu, J., Xue, C., Hu, G., Yu, M., Chen, Y., Zhang, L., Zhang, W., Hu, X., Sun, Y., Liu, W., & Chen, J. (2022). Differential functional connectivity of insular subdivisions in de novo Parkinson's disease with mild cognitive impairment. *Brain Imaging and Behavior*, *16*(1), 1–10. https://doi.org/10.1007/s11682-021-00471-2

Panman, J. L., Jiskoot, L. C., Bouts, M., Meeter, L. H. H., van der Ende, E. L., Poos, J. M., Feis, R. A., Kievit, A. J. A., van Minkelen, R., Dopper, E. G. P., Rombouts, S., van Swieten, J. C., & Papma, J. M. (2019). Gray and white matter changes in presymptomatic genetic frontotemporal dementia: A longitudinal MRI study. *Neurobiology of Aging*, *76*, 115–124. https://doi.org/10.1016/j.neurobiolaging.2018.12.017

Paquola, C., Vos De Wael, R., Wagstyl, K., Bethlehem, R. A. I., Hong, S. J., Seidlitz, J., Bullmore, E. T., Evans, A. C., Misic, B., Margulies, D. S., Smallwood, J., & Bernhardt, B. C. (2019). Microstructural and functional gradients are increasingly dissociated in transmodal cortices. *PLoS Biology*, *17*(5), e3000284. https://doi.org/10.1371/journal.pbio.3000284

Perez Diaz, M., Pochon, J. B., Ghahremani, D. G., Dean, A. C., Faulkner, P., Petersen, N., Tyndale, R. F., Donis, A., Paez, D., Cahuantzi, C., Hellemann, G. S., & London, E. D. (2021). Sex differences in the Association of Cigarette Craving with Insula Structure. *The International Journal of Neuropsychopharmacology*, *24*(8), 624–633. https://doi.org/10.1093/ijnp/pyab015

Poldrack, R. A., Congdon, E., Triplett, W., Gorgolewski, K. J., Karlsgodt, K. H., Mumford, J. A., Sabb, F. W., Freimer, N. B., London, E. D., Cannon, T. D., & Bilder, R. M. (2016). A phenome-wide examination of neural and cognitive function. *Scientific Data*, *3*, 160110. https://doi.org/10.1038/sdata.2016.110

Qi, Z., Wang, J., Gong, J., Su, T., Fu, S., Huang, L., & Wang, Y. (2022). Common and specific patterns of functional and structural brain alterations in schizophrenia and bipolar disorder: A multimodal voxel-based meta-analysis. *Journal of Psychiatry & Neuroscience*, *47*(1), E32–E47. https://doi.org/10.1503/jpn.210111

Qiu, Z., & Wang, J. (2021). Altered neural activities during response inhibition in adults with addiction: A voxel-wise meta-analysis. *Psychological Medicine*, *51*(3), 387–399. https://doi.org/10.1017/S0033291721000362

Royer, J., Paquola, C., Lariviere, S., Vos de Wael, R., Tavakol, S., Lowe, A. J., Benkarim, O., Evans, A. C., Bzdok, D., Smallwood, J., Frauscher, B., & Bernhardt, B. C. (2020). Myeloarchitecture gradients in the human insula: Histological underpinnings and association to intrinsic functional connectivity. *NeuroImage*, *216*, 116859. https://doi.org/10.1016/j.neuroimage.2020.116859

Sheffield, J. M., Rogers, B. P., Blackford, J. U., Heckers, S., & Woodward, N. D. (2020). Insula functional connectivity in schizophrenia. *Schizophrenia Research*, *220*, 69–77. https://doi.org/10.1016/j.schres.2020.03.068

Shine, J. M., Breakspear, M., Bell, P. T., Ehgoetz Martens, K. A., Shine, R., Koyejo, O., Sporns, O., & Poldrack, R. A. (2019). Human cognition involves the dynamic integration of neural activity and neuromodulatory systems. *Nature Neuroscience*, *22*(2), 289–296. https://doi.org/10.1038/s41593-018-0312-0

Taylor, K. S., Seminowicz, D. A., & Davis, K. D. (2009). Two systems of resting state connectivity between the insula and cingulate cortex. *Human Brain Mapping*, *30*(9), 2731–2745. https://doi.org/10.1002/hbm.20705

Tian, Y., & Zalesky, A. (2018). Characterizing the functional connectivity diversity of the insula cortex: Subregions, diversity curves and behavior. *NeuroImage*, *183*, 716–733. https://doi.org/10.1016/j.neuroimage.2018.08.055

Tian, Y., Zalesky, A., Bousman, C., Everall, I., & Pantelis, C. (2019). Insula functional connectivity in schizophrenia: Subregions, gradients, and symptoms. *Biological Psychiatry: Cognitive Neuroscience and Neuroimaging*, *4*(4), 399–408. https://doi.org/10.1016/j.bpsc.2018.12.003

Tremblay, C., Abbasi, N., Zeighami, Y., Yau, Y., Dadar, M., Rahayel, S., & Dagher, A. (2020). Sex effects on brain structure in de novo Parkinson's disease: A multimodal neuroimaging study. *Brain*, *143*(10), 3052–3066. https://doi.org/10.1093/brain/awaa234

Turel, O., He, Q., Wei, L., & Bechara, A. (2021). The role of the insula in internet gaming disorder. *Addiction Biology*, *26*(2), e12894. https://doi.org/10.1111/adb.12894

Uddin, L. Q., Kinnison, J., Pessoa, L., & Anderson, M. L. (2014). Beyond the tripartite cognition-emotion-interoception model of the human insular

cortex. *Journal of Cognitive Neuroscience*, 26(1), 16–27. https://doi.org/10.1162/jocn_a_00462

Uddin, L. Q., & Menon, V. (2009). The anterior insula in autism: Under-connected and under-examined. *Neuroscience and Biobehavioral Reviews*, 33(8), 1198–1203. https://doi.org/10.1016/j.neubiorev.2009.06.002

Uddin, L. Q., Nomi, J. S., Hebert-Seropian, B., Ghaziri, J., & Boucher, O. (2017). Structure and function of the human insula. *Journal of Clinical Neurophysiology*, 34(4), 300–306. https://doi.org/10.1097/WNP.0000000000000377

Calhoun, V. D., Adali, T., Pearlson, G. D., & Pekar, J. J. (2001). A method for making group inferences from functional MRI data using independent component analysis. *Human Brain Mapping*, 14(3), 140–151. https://doi.org/10.1002/hbm.1048

Vogel, J. W., La Joie, R., Grothe, M. J., Diaz-Papkovich, A., Doyle, A., Vachon-Presseau, E., Lepage, C., Vos de Wael, R., Thomas, R. A., Iturria-Medina, Y., Bernhardt, B., Rabinovici, G. D., & Evans, A. C. (2020). A molecular gradient along the longitudinal axis of the human hippocampus informs large-scale behavioral systems. *Nature Communications*, 11(1), 960. https://doi.org/10.1038/s41467-020-14518-3

Vos de Wael, R., Benkarim, O., Paquola, C., Lariviere, S., Royer, J., Tavakol, S., Xu, T., Hong, S. J., Langs, G., Valk, S., Misic, B., Milham, M., Margulies, D., Smallwood, J., & Bernhardt, B. C. (2020). BrainSpace: A toolbox for the analysis of macroscale gradients in neuroimaging and connectomics datasets. *Communications Biology*, 3(1), 103. https://doi.org/10.1038/s42003-020-0794-7

Vos de Wael, R., Lariviere, S., Caldairou, B., Hong, S. J., Margulies, D. S., Jefferies, E., Bernasconi, A., Smallwood, J., Bernasconi, N., & Bernhardt, B. C. (2018). Anatomical and microstructural determinants of hippocampal subfield functional connectome embedding. *Proceedings of the National Academy of Sciences of the United States of America*, 115(40), 10154–10159. https://doi.org/10.1073/pnas.1803667115

Wagstyl, K., Ronan, L., Goodyer, I. M., & Fletcher, P. C. (2015). Cortical thickness gradients in structural hierarchies. *NeuroImage*, 111, 241–250. https://doi.org/10.1016/j.neuroimage.2015.02.036

Wei, D., Zhuang, K., Ai, L., Chen, Q., Yang, W., Liu, W., Wang, K., Sun, J., & Qiu, J. (2018). Structural and functional brain scans from the cross-sectional Southwest University adult lifespan dataset. *Scientific Data*, 5, 180134. https://doi.org/10.1038/sdata.2018.134

Wei, L., Zhang, S., Turel, O., Bechara, A., & He, Q. (2017). A tripartite neurocognitive model of internet gaming disorder. *Frontiers in Psychiatry*, 8, 285. https://doi.org/10.3389/fpsyt.2017.00285

Wysiadecki, G., Malkiewicz, A., Rozniecki, J., Polguj, M., Haladaj, R., Zytkowski, A., & Topol, M. (2018). Anatomical variations of the insular gyri: A morphological study and proposal of unified classification. *Clinical Anatomy*, 31(3), 347–356. https://doi.org/10.1002/ca.23060

Xu, X., Li, Q., Qian, Y., Cai, H., Zhang, C., Zhao, W., Zhu, J., & Yu, Y. (2022). Genetic mechanisms underlying gray matter volume changes in patients with drug-naive first-episode schizophrenia. *Cerebral Cortex*, bhac211. https://doi.org/10.1093/cercor/bhac211

Yan, C. G., Wang, X. D., Zuo, X. N., & Zang, Y. F. (2016). DPABI: Data processing & analysis for (resting-state) brain imaging. *Neuroinformatics*, 14(3), 339–351. https://doi.org/10.1007/s12021-016-9299-4

Yang, S., Meng, Y., Li, J., Li, B., Fan, Y. S., Chen, H., & Liao, W. (2020). The thalamic functional gradient and its relationship to structural basis and cognitive relevance. *NeuroImage*, 218, 116960. https://doi.org/10.1016/j.neuroimage.2020.116960

Yu, H., Li, M. L., Li, Y. F., Li, X. J., Meng, Y., Liang, S., Li, Z., Guo, W., Wang, Q., Deng, W., Ma, X., Coid, J., & Li, D. T. (2020). Anterior cingulate cortex, insula and amygdala seed-based whole brain resting-state functional connectivity differentiates bipolar from unipolar depression. *Journal of Affective Disorders*, 274, 38–47. https://doi.org/10.1016/j.jad.2020.05.005

Zhao, H., Turel, O., Bechara, A., & He, Q. (2022). How distinct functional insular subdivisions mediate interacting neurocognitive systems. *Cerebral Cortex*, bhac169. https://doi.org/10.1093/cercor/bhac169

Zhu, J., Zhang, S., Cai, H., Wang, C., & Yu, Y. (2020). Common and distinct functional stability abnormalities across three major psychiatric disorders. *Neuroimage Clinical*, 27, 102352. https://doi.org/10.1016/j.nicl.2020.102352

Zhu, J., Zhu, D. M., Qian, Y., Li, X., & Yu, Y. (2018). Altered spatial and temporal concordance among intrinsic brain activity measures in schizophrenia. *Journal of Psychiatric Research*, 106, 91–98. https://doi.org/10.1016/j.jpsychires.2018.09.015

Zhu, J., Zhuo, C., Qin, W., Xu, Y., Xu, L., Liu, X., & Yu, C. (2015). Altered resting-state cerebral blood flow and its connectivity in schizophrenia. *Journal of Psychiatric Research*, 63, 28–35. https://doi.org/10.1016/j.jpsychires.2015.03.002

Zhu, J., Zhuo, C., Xu, L., Liu, F., Qin, W., & Yu, C. (2017). Altered coupling between resting-state cerebral blood flow and functional connectivity in schizophrenia. *Schizophrenia Bulletin*, 43(6), 1363–1374. https://doi.org/10.1093/schbul/sbx051

Zhuo, C., Zhu, J., Qin, W., Qu, H., Ma, X., & Yu, C. (2017). Cerebral blood flow alterations specific to auditory verbal hallucinations in schizophrenia. *The British Journal of Psychiatry*, 210(3), 209–215. https://doi.org/10.1192/bjp.bp.115.174961

Zhuo, C., Zhu, J., Wang, C., Qu, H., Ma, X., & Qin, W. (2017). Different spatial patterns of brain atrophy and global functional connectivity impairments in major depressive disorder. *Brain Imaging and Behavior*, 11(6), 1678–1689. https://doi.org/10.1007/s11682-016-9645-z

SUPPORTING INFORMATION

Additional supporting information can be found online in the Supporting Information section at the end of this article.